VIIRS/J1 Polarization Narrative

Eugene Waluschka[1], Joel McCorkel[1], Jeff McIntire[2], David Moyer[3], Brendan McAndrew[1], Steven W. Brown[4], Keith R. Lykke[4], James B. Young[5], Eric Fest[6], James Butler[1], Tung R. Wang[7], Eslim O. Monroy[7], Kevin Turpie[8], Gerhard Meister[1] and Kurtis J.Thome[1]

[1]NASA/Goddard Space Flight Center, Greenbelt, MD
[2]Science Systems and Applications, Inc., Greenbelt, MD
[3]The Aerospace Corporation, El Segundo, CA
[4]NIST, Gaithersburg, MD
[5]Stellar Solutions, Palo Alto, CA
[6]Raytheon, Tucson, AZ
[7]Raytheon, El Segundo, CA
[8]University of Maryland, Baltimore County, Baltimore, MD

ABSTRACT

The polarization sensitivity of the Visible/NearIR (VISNIR) bands in the Joint Polar Satellite Sensor 1 (J1) Visible Infrared Imaging Radiometer Suite (VIIRS) instrument was measured using a broadband source. While polarization sensitivity for bands M5-M7, I1, and I2 was less than 2.5 %, the maximum polarization sensitivity for bands M1, M2, M3, and M4 was measured to be 6.4 %, 4.4 %, 3.1 %, and 4.3 %, respectively with a polarization characterization uncertainty of less than 0.38%. A detailed polarization model indicated that the large polarization sensitivity observed in the M1 to M4 bands is mainly due to the large polarization sensitivity introduced at the leading and trailing edges of the newly manufactured VISNIR bandpass focal plane filters installed in front of the VISNIR detectors. This was confirmed by polarization measurements of bands M1 and M4 bands using monochromatic light. Discussed are the activities leading up to and including the two polarization tests, some discussion of the polarization model and the model results, the role of the focal plane filters, the polarization testing of the Aft-Optics-Assembly, the testing of the polarizers at the National Aeronautics and Space Administration's (NASA) Goddard center and at the National Institute of Science and Technology (NIST) facility and the use of NIST's Traveling Spectral Irradiance and Radiance responsivity Calibrations using Uniform Sources (T-SIRCUS) for polarization testing and associated analyses and results.

Keywords: JPSS, VIIRS, T-SIRCUS, polarization

1. INTRODUCTION

The VISNIR bands polarization sensitivity of Joint Polar Satellite Sensor (JPSS) VIIRS/J1[1] instrument was measured using a broadband source. While polarization sensitivity for bands M5-M7, I1, and I2 was less than 2.5 %, (the requirement is bands M1, I2, M7 less than 3 % and bands M2, M3, M4, I1, M5, M6 less than 2.5 %) the polarization sensitivity for bands M1, M2, M3, and M4 was measured to be 6.4 %, 4.4 %, 3.1 %, and 4.3 %, respectively with a polarization characterization standard uncertainty less than 0.38 %. The expectation was that VIIRS/J1 would, as did VIIRS/SNNP[2,3,4] (on the Suomi National Polar-orbiting Partnership – SNPP), meet its polarization requirements. The unexpectedly large polarization sensitivity resulted in the following activities:

- determine the root cause of the increased polarization sensitivity using a detailed polarization ray trace model (using the commercial code FRED™ from Photon Engineering);
- determine by means of the polarization ray trace model that the increased polarization sensitivity was due to the focal plane filters leading and trailing spectral bandpass edges which differed from VIIRS/SNNP;
- find ways to ascertain the correctness of the models predictions and the need to develop an understanding of the uncertainty of the measurements;
- repeat a subset of the original polarization measurements including new telescope scan angles to estimate "scan angle" interpolation errors;

Earth Observing Systems XX, edited by James J. Butler, Xiaoxiong (Jack) Xiong,
Xingfa Gu, Proc. of SPIE Vol. 9607, 960712 · © 2015 SPIE
CCC code: 0277-786X/15/$18 · doi: 10.1117/12.2190138

- perform a series of polarization measurements using monochromatic light provided by NIST's T-SIRCUS tunable lasers to verify the model's predictions.

The following sections describe briefly, in somewhat chronological order, the activities associated with the polarization measurements, the results and the analysis of the observed polarization sensitivity of VIIRS/J1.

For historical reasons, the VIIRS program uses some non-standard terminology when referring to the polarization sensitivity of the system. The translation between VIIRS and standard Mueller matrix terminology[5] is given in Table A1.

2. VISNIR OPTICAL PATH

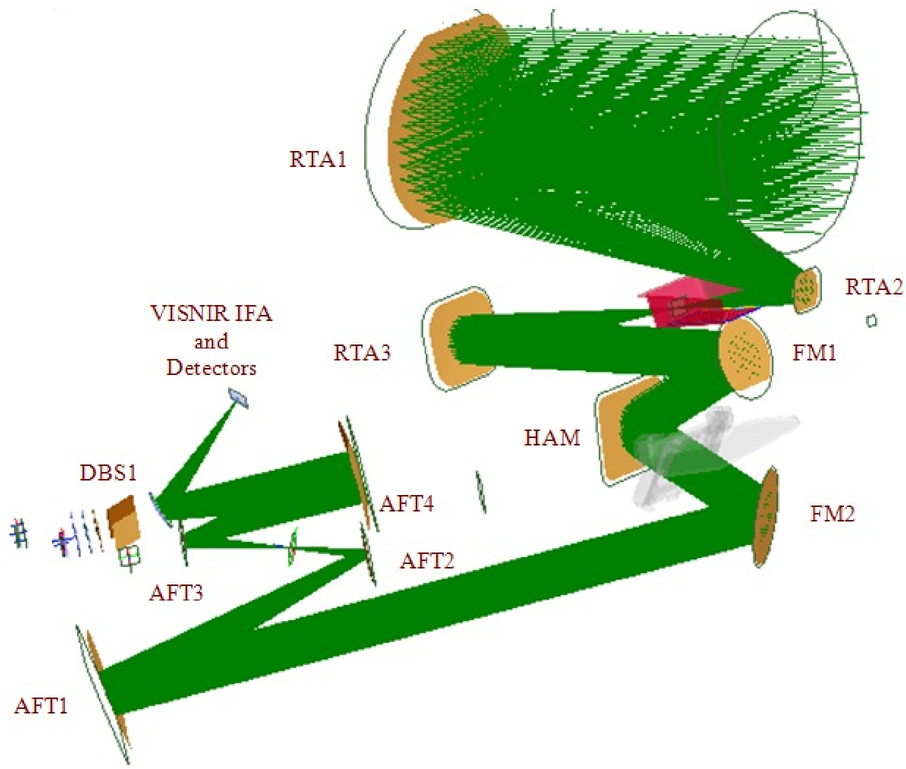

Figure 1: VISNIR optics within the VIIRS/J1 FRED model

To orient the reader to subsequent sections we start with the VIIRS VISNIR optics, shown in Fig. 1. The rotating telescope (a cross track scanner) consists of three powered elements, RTA1, RTA2, RTA3 and a flat fold mirror (FM1) which directs the light onto the rotating "half-angle" mirror (HAM), which is a two sided rotating fold mirror. The half angle mirror, rotating at half the speed of the telescope de-rotates the light beam and directs it onto the aft-optics. It should be noted that the HAM is the only optic with a varying – during scanning – angle of incidence; hence it is the only optic which can change the polarization sensitivity during scanning! The aft-optics assembly (AOA) consists of the four powered elements, AFT1 to AFT4 followed by the dichroic #1 (DBS1) which reflects the visible and near-IR light toward the VISNIR/DNB (Day Night Band) focal plane filter assembly which is immediately above the detectors. The image on the focal plane is about the size of a 35 mm slide.

3. AFT-OPTICS-ASSEMBLY (AOA) POLARIZATION TEST

The polarization sensitivity of the VIIRS/J1 AOA was measured in the fourth quarter of 2012[6,7,8]. This was motivated by the fact that VIIRS/SNNP instrument level polarization measurements performed[3] in 2009 had showed that, even though the instrument met its polarization requirement, there was non-negligible detector-to-detector (d2d) variation in polarization sensitivities in bands M1 and M4. Subsequent testing confirmed that the d2d variation was real and the test approach and equipment were not the source of the observed d2d variation. This d2d variation, if it is real, would require a separate atmospheric correction for each detector and not a single correction applied to all of the detectors in a spectral band. Polarization ray trace modeling of VIIRS/SNNP was performed but the results were inconclusive as to the cause of the d2d variation. By performing the polarization sensitivity measurement on the AOA, where fewer optical elements were involved than in sensor-level testing, would help to identify which optical element(s) could cause a d2d variation in the VIIRS/J1 instrument. (*DoLP* is defined in the appendix.)

The AOA polarization sensitivity measurement was performed with following arrangement: the AOA was looking into a Spherical Integrating Sphere (SIS) with a polarizer in-between, i.e.:

Spherical Integrating Source => polarizer(theta) => AOA

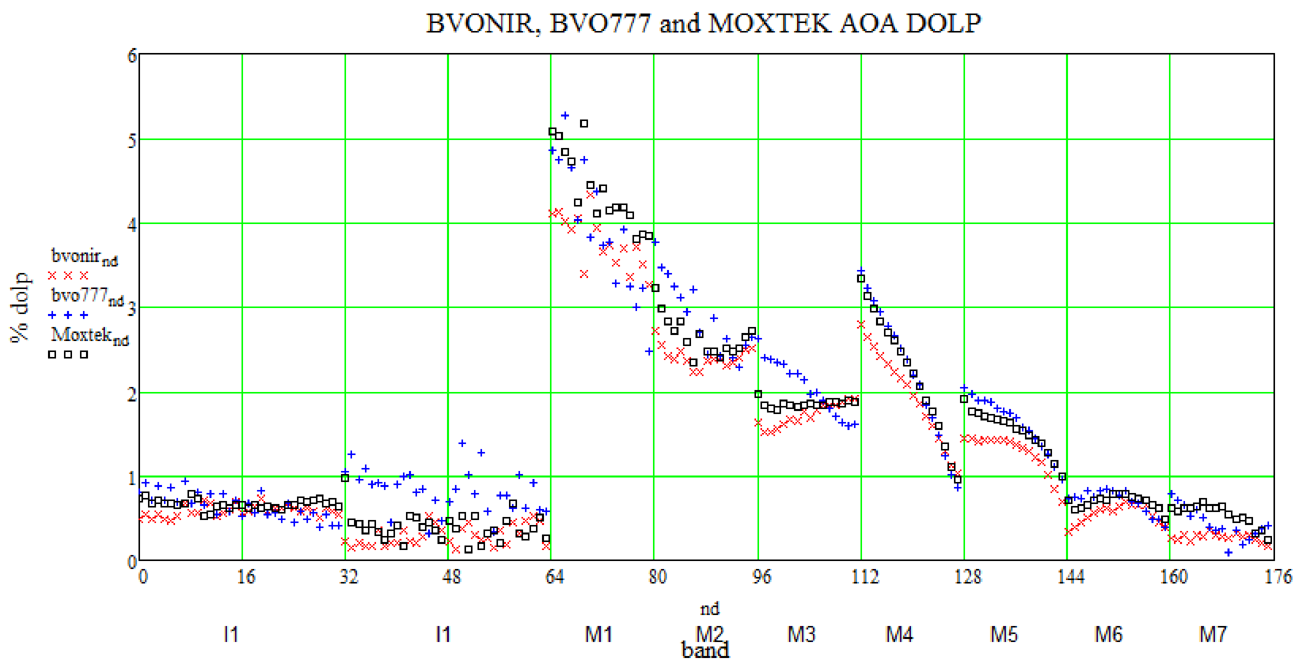

Figure 2: Abscissa indicates (band and 16 detectors for M bands and 32 detectors for I bands) and ordinate is % $DoLP=sqrt(A2^2+B2^2)$

Three polarizers were used: Bolder Vision Optik's[9] BVO777™ and BVONIR™ sheet polarizers, and a 15.24cm (6") diameter Moxtek[10] wire grid polarizer. All polarizers covered the AOA entrance aperture. The polarizers were rotated from 0 to 360 degrees in 15 degree steps. From the resulting two theta intensity variation, the sensitivity of the AOA to linearly polarized light, i.e. AOA Degree of Linear Polarization (*DoLP*) was determined. Each polarizer measurement was performed twice; by-and-large the measurements repeated well considering the magnitude of the random noise which was more of a factor when the two theta sinusoidal variations were small. The BVONIR™ and BVO777™ measurements were corrected for polarization efficiency determined by cross polarization measurement of two polarizers of the same type, one fixed and one rotating, where the AOA is used as a detector. (For some of the BVO777 measurements a Sonoma[11] long wave blocking filter was used to reduce the possible IR leakage for bands M1 to M3.) The Moxtek efficiency was not measured since its' polarization efficiency was deemed high. As shown in Fig. 2, the results using the Moxtek wire polarizer, even without the polarization efficiency correction, were in line with the corrected sheet polarizer measurements.

The three sets of data plotted in Fig. 2 show results of the measurements using the BVONIR™ sheet, the BVO777™ sheet and the Moxtek wire grid polarizer. Each point in the plot is an averaged detector response from two repeated measurements. All three polarizers give reasonably consistent result for all of the bands. The I1 and I2 bands (32 detectors) exhibited the most noise because the two theta variation was small. Band M1 and M4 show a pronounced d2d variation. Band M1, even though it has the most polarization sensitivity, between 3 and 5 percent, was inexplicably noisy.

Due to the concern that BOVNIR™ polarization sensitivity measurement might be contaminated by stray light (possibly from the polarizer itself), these AOA results was not viewed as representative of the system level polarization sensitivity.

4. REASON FOR POLARIZATION REQUIREMENT

The instrument response is required to vary less than 2.5 % when viewing fully polarized light being measured for all reflective solar bands, except I2, M1 and M7, for which the requirement criterion is set at 3 %[12]. The degree of polarization from molecular scattering for VISNIR light observed above the atmosphere can be as high as 60 % to 70 %, depending on the wavelength. The resulting variation in instrument response can thus be greater than 1.5 % (or 2 % in the case of band M1). This creates geometrically dependent artifacts in the satellite imagery for science data products that are sensitive to radiometric errors. In particular, retrieval of band-specific, water-column reflectance below the air-water interface, or ocean color remote sensing reflectance, is sensitive enough to require a correction, based on laboratory characterization of the instrument polarization response, to the Top-of-Atmosphere (TOA) radiance or reflectance measurements.

This correction is essential to calculating accurate ocean color remote sensing reflectance (or water-leaving radiance), from which all traditional ocean color data products are derived. Without this correction, the ocean data products would show strong scan dependent biases and striping that would vary seasonally and hemispherically across the globe. Previous experience with Moderate Resolution Imaging Spectroradiometer (MODIS) Aqua showed that this could also impact global and synoptic trends, thus adversely affecting these products as climate data records.

Both the National Oceanic and Atmospheric Administration (NOAA) and the National Aeronautics and Space Administration (NASA) ocean color processing systems have the capability of apply this correction to the ocean products NOAA Environmental Data Records (EDR) or NASA Level-2 products, respectively) through the correction factor p_c, defined as

$$p_c = \frac{L_m}{L_t} \qquad \text{Eq. 1}$$

where L_m and L_t are defined as the measured and true TOA radiance, respectively. For most scan angles, p_c can be calculated as

$$p_c = \frac{1}{1 - m_{12} Q_t / L_m - m_{13} U_t / L_m} \qquad \text{Eq. 2}$$

where Q_t and U_t are the modeled Stokes Vector components of the TOA radiance associated with molecular scatter. For scan angles close to nadir, a matrix rotation is needed, as described by Eq. 5 in Meister et al.[13]. This method has been employed for ocean color for a long time and experience with it is extensive. Gordon et al.[14] originally developed this correction approach, and its implementation is practically identical for both MODIS and VIIRS/SNPP (except, of course, for the values of the coefficients m_{12} and m_{13}, which are derived from the prelaunch characterization of the respective instruments). The polarization response correction is applied to the TOA radiance during NOAA EDR or NASA Level-2 processing because of the availability of Rayleigh scatter model being used in the atmospheric correction.

5. WORK AT NIST AND GODDARD CHARACTERIZING POLARIZERS

The BVO777™ and BVONIR™ sheet polarizers were used to measure the VIIRS/SNNP/J1 polarization sensitivity. The large area of the sheet polarizers enables the required full aperture polarization testing. From polarizer efficiency considerations, for the VIIRS/SNNP measurements, the BVO777™ was preferred over the BVONIR™ polarizer for the shorter wavelengths, although both produced similar results over all of the VISNIR wavelength during instrument-level tests and in the preliminary tests, at Raytheon, measuring the polarization of a tilted glass plate, albeit with different measurement uncertainties. However, the BVO777™ has a small polarization efficiency at M7/I2 bands and BVONIR™ is preferred at these wavelengths.

The appearance of the BVO777™ sheet is clear and it does not put any great requirements on the shape or alignment of the circular exit aperture of the SIS. The BVONIR™ sheet polarizer, in contrast is white and diffuse in appearance and it does require that the SIS aperture be circular (because of the asymmetric scattering of light) and aligned with the optical axes of the SIS and VIIRS. The AOA polarization test used a smaller diameter integrating sphere with a circular aperture, than that used for the instrument level tests.

Several polarizing elements were characterized at Goddard in order to verify that the expected polarization signal can be retrieved using a monochromatic source. The recent (last couple of years) VIIRS-related polarizer efficiency measurements were performed at Goddard and NIST. The typical measurement setup is:

SIS => limiting aperture => polarizer-1(fixed) => polarizer-2(theta) => spectral filter => detector =>sinusoidal variation

The SIS's light source has been incandescent bulbs or a fiber connected to a monochromatic light source such as the SIRCUS laser. The simplest measurement has both polarizers 1 and 2 of the same type (i.e. BVONIR™ and BVONIR™ or Moxtek and Moxtek) as this approach does not require knowledge of the SIS radiance as long as it remains stable or accurately monitored. Another measurement approach is to have polarizer-1 be one with a very high extinction ratio. Either approach gives the sinusoidal signal from which the correction factor or extinction ratio is determined. The results of the tests were consistent with the VIIRS/SNNP polarizer characterization, and therefore provided confidence that the BVONIR™ polarizer could be used to characterize the polarization sensitivity of VIIRS/J1 to required levels of accuracy using a monochromatic source.

For those who have followed the MODIS polarization testing and remember the observed "4 theta" sinusoidal variation[15], the cause of which was the light, due to telecentricity, reflected from the focal plane back through all of the MODIS optics, into the Polarization Source Assembly reflecting from the back of the Ahrens prism (hence polarized again) and then back into MODIS and producing the not so small "4 theta" variation. This same 4 theta variation was observed in the Moxtek – Moxtek efficiency tests when the separation was small and caused by the light bouncing between the two polarizers.

6. POLARIZATION TEST SETUP, SPECIAL TEST EQUIPMENT (STE) RESIDUAL POLARIZATION AND POLARIZATION CHARACTERIZATION UNCERTAINTY

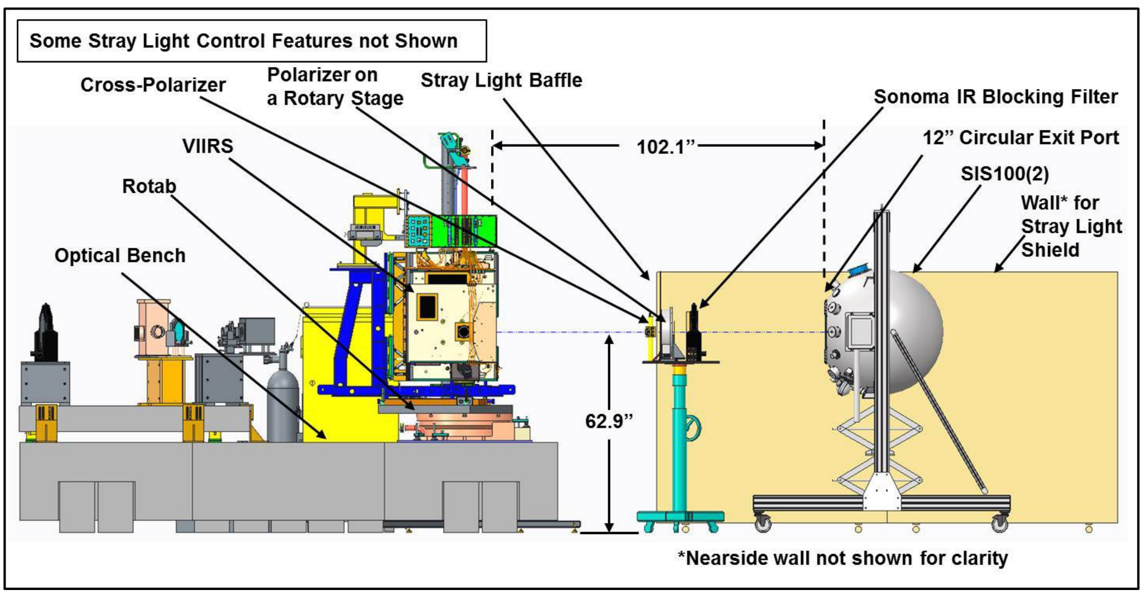

Figure 3: VIIRS polarization test setup

The VIIRS polarization test setup for FP-11, FP-11' and T-SIRCUS is shown in Fig. 3. The VIIRS sensor was mounted on a Rotating table (Rotab) such that it could be rotated in its scan plane and have the scan angle set anywhere in-between -55° to +55° from nadir. Unpolarized light from the SIS was transmitted through a 27.94cm (11”) diameter BVONIR™ or BVO777™ sheet polarizer producing linearly polarized light. The sheet polarizer mounted to a Newport (RV350PE) rotary stage, tilted 0.6° toward the gravity, was rotated from 0° to 360° (or 0° to 180° for the T-SIRCUS test) in 15° increments. For the shorter wavelength bands (488nm), a long-wave blocking filter, Sonoma C165-210-JB, was located between the SIS and the polarizer to block wavelengths longer than about 600nm. The VIIRS line-of-sight (LOS), sheet polarizer, Sonoma filter, and SIS were co-aligned in both positions and angles. A stray light baffle was installed, as shown, in between the SIS and VIIRS, to minimize possible stray light not directly illuminated through the sheet polarizer. Additional baffle walls and Velostat sheets were used to enclose the sheet polarizer and SIS setup to suppress stray light. For the FP-11 and FP-11’ tests, a 101.6cm (40”) diameter SIS(100)-2 with a 30.48cm (12”) circular exit port was used to generate a white light illumination. For the T-SIRCUS polarization test the SIS(100)-2 was replaced by a 101.6cm (40”) diameter T-SIRCUS SIS which also had a 30.48cm (12”) circular exit port. The *in-situ* stray light characterization was performed by collecting data with the SIS on and off and with an obscuration test (A.K.A. the lollipop which entails placing a circular disk, slightly larger than the VIIRS footprint at the polarizer, in front of the sheet polarizer).

STE Characterization Uncertainties (%)

M1	M2	M3	M4	M5	M6	M7	I1	I2
0.14	0.12	0.14	0.10	0.13	0.09	0.10	0.20	0.10

RSS

Measured Tilted Plate Polarization Error (%)

M1	M2	M3	M4	M5	M6	M7	I1	I2
0.14	0.12	0.14	0.10	0.12	0.08	0.09	0.19	0.09

Tilted Plate Measurement Uncertainty (%)

M1	M2	M3	M4	M5	M6	M7	I1	I2
0.02	0.02	0.01	0.02	0.03	0.02	0.03	0.06	0.03

Residual Polarization/Modulation STE (%)

M1	M2	M3	M4	M5	M6	M7	I1	I2
0.02	0.02	0.02	0.01	0.01	0.01	0.01	0.01	0.01

Tilted Plate to Gravity Angle Uncertainty (%)

M1	M2	M3	M4	M5	M6	M7	I1	I2
0.001								

Tilted Plate Polarization Uncertainties in Prediction (%)

M1	M2	M3	M4	M5	M6	M7	I1	I2
0.02								

RSS

Tilted Plate Angle Uncertainty (%)

M1	M2	M3	M4	M5	M6	M7	I1	I2
0.02								

Tilted Plate Model Uncertainty (%)

M1	M2	M3	M4	M5	M6	M7	I1	I2
0.001								

Fused Silica Index of Refraction Uncertainty (%)

M1	M2	M3	M4	M5	M6	M7	I1	I2
0.001								

Note: All Numbers Express As Percentages (eg: 0.24 = 0.24%)

Table 1: STE residual polarization

The polarizer sheet efficiency was measured by adding a second, non-rotating sheet polarizer in the optical path and in front of the rotating polarizer, Fig. 3. The polarizer efficiency test was performed for each sheet polarizer type with both the rotating and non-rotating polarizers being of the same type (i.e. BVO777™ with BVO777™ and BVONIR™ with BVONIR™).

In the FP-11 and FP-11’ tests, for bands M1 to M3 the polarization sensitivity was based on measurements using the BVONIR™ polarizer plus Sonoma IR blocking filter. For the other VISNIR bands, the results are based only the BVONIR™ polarizer. For the T-SIRCUS bands M1 and M4 polarization tests, only the BVONIR™ sheet polarizer was used without Sonoma IR blocking filter since T-SIRCUS generates monochromatic light and there is no need to block the longer wavelengths.

Prior to FP-11 and FP-11’ polarization tests, the residual polarization of the testing optics and light source was characterized using the Polarization Test Source Assembly (PTSA) which was mounted on the Rotab in place of VIIRS.

The PTSA was designed to have a similar acceptance aperture and effective focal length as VIIRS, with VISNIR band pass filter witness samples placed in front of the PTSA detector to simulate VISNIR band performance.

An additional check on the polarization measurement approach shown in Fig. 3 , but with VIIRS replaced by the PTSA (and by similarity to the actual VIIRS measurement), the polarization sensitivity of a 30.48cm (12”) diameter fused silica plate, tilted 30^o relative to the VIIRS-polarizer line-of-sight, was measured. The tilted glass plate was placed in-between the PTSA and the polarizer and data collected as the polarizer was rotated. Data was also collected with PTSA tilted to +0.75 mR and -0.75mR in the VIIRS track direction to simulate the VIIRS VISNIR detector spatial dependent polarization sensitivity. The measurements and analysis showed that for the VIIRS VISNIR bands the PTSA based polarization measurement uncertainty varied from 0.09 % at M6 band and to 0.2 % at I1 band, Table 2.

Table 2 shows both estimated 1σ rms and worst case (maximum) polarization uncertainties. The worst case (maximum) uncertainty for VIIRS instrument measurements varied from 0.13 % for M6 band and to 0.38 % for band M1. These uncertainties meet the polarization characterization 1σ uncertainty requirement of 0.5 % with margin.

Polarization Characterization Uncertainties (%)

	M1	M2	M3	M4	M5	M6	M7	I1	I2
A: worst-case (max)	0.38	0.30	0.20	0.22	0.19	0.13	0.14	0.29	0.36
B: 1σ rms	0.25	0.22	0.17	0.16	0.15	0.10	0.12	0.23	0.22

RSS

STE Characterization Uncertainties (%)

	M1	M2	M3	M4	M5	M6	M7	I1	I2
B	0.14	0.12	0.14	0.10	0.13	0.09	0.10	0.20	0.10

Characterization Uncertainties from VIIRS Test (%)

	M1	M2	M3	M4	M5	M6	M7	I1	I2
A	0.35	0.27	0.14	0.19	0.14	0.10	0.10	0.21	0.35
B	0.21	0.18	0.09	0.12	0.08	0.06	0.07	0.11	0.20

RSS

Measurement Repeatability (%)

	M1	M2	M3	M4	M5	M6	M7	I1	I2
A	0.019	0.012	0.020	0.030	0.009	0.008	0.008	0.019	0.007
B	0.014	0.010	0.012	0.014	0.007	0.007	0.006	0.008	0.005

Scan Angle Interpolation (%)

	M1	M2	M3	M4	M5	M6	M7	I1	I2
A	0.07	0.04	0.05	0.10	0.08	0.07	0.06	0.07	0.06
B	0.03	0.02	0.02	0.04	0.04	0.04	0.02	0.03	0.02

Additional Stray Light of VIIRs Test (%)

	M1	M2	M3	M4	M5	M6	M7	I1	I2
A	0.0024	0.0010	0.0004	0.0036	0.0019	0.0007	0.0009	0.0006	0.0004
B	0.0010	0.0006	0.0002	0.0019	0.0009	0.0004	0.0004	0.0003	0.0001

Polarization Efficiency Correction Uncertainty (%)

	M1	M2	M3	M4	M5	M6	M7	I1	I2
A	0.10	0.07	0.05	0.06	0.03	0.02	0.02	0.02	0.02
B	0.07	0.05	0.04	0.04	0.02	0.01	0.01	0.01	0.01

VIIRS to Gravity Angle Uncertainty (%)

	M1	M2	M3	M4	M5	M6	M7	I1	I2
A	0.0008	0.0006	0.0004	0.0006	0.0003	0.0002	0.0002	0.0001	0.0002
B	0.0008	0.0005	0.0004	0.0005	0.0003	0.0001	0.0001	0.0001	0.0001

Out-of-Band Response (%)

	M1	M2	M3	M4	M5	M6	M7	I1	I2
A	0.06	0.25	0.09	0.13	0.07	0.06	0.07	0.04	0.34
B	0.04	0.17	0.07	0.10	0.03	0.04	0.06	0.03	0.20

SIS to Top of Atmosphere Spectrum Uncertainty (%)

	M1	M2	M3	M4	M5	M6	M7	I1	I2
A	0.33	0.06	0.08	0.08	0.09	0.01	0.03	0.2	0.03
B	0.19	0.04	0.05	0.04	0.06	0.01	0.02	0.10	0.02

A: Worst Case (max)
B: 1σ rms

Note: All Numbers Express As Percentages
(eg: 0.24 = 0.24%)

Table 2: VIIRS polarization characterization uncertainty (k=1)

7. FIRST POLARIZATION TEST FP-11

The first VIIRS/J1 polarization test, FP-11[16] , took place at Raytheon Space and Airborne System (SAS) in El Segundo in the 4th quarter of 2013. Testing was performed with the room lights turned off. As shown in Fig. 3, with VIIRS looking into the SIS(100)-2, at scan angles of -55^o, -45^o, -20^o, -8^o, +22^o, +45^o, and +55^o, the polarizer was rotated from 0^o to 360^o in 15^o steps. At each polarizer angle, the detector data in each VISNIR band was recorded. The detector data vs. polarizer angle shows a distinctive “2 theta” sinusoidal variation. Fitting a 2 theta sinusoid to this data gives the needed Mueller matrix components from which we get, for each detector, the *DoLP*’s which are plotted in Fig. 4 A comparison of the FP-11 and AOA results, Fig. 2 and Fig. 4, shows that, even though there is no telescope and HAM in the AOA, the polarization sensitivity results are similar. The AOA data seems noiser and was about ½ percent less than the FP-11 results. Fig. 4(a) and 4(b) show the polarization sensitivity variation with scan angle and the HAM side differences. While band M1 detector 1 shows very little scan angle variation, detector 16 shows about 4 % scan angle variation. As can be seen in Fig. 4, bands M1, M2, M3, and M4 exceed the polarization requirement.

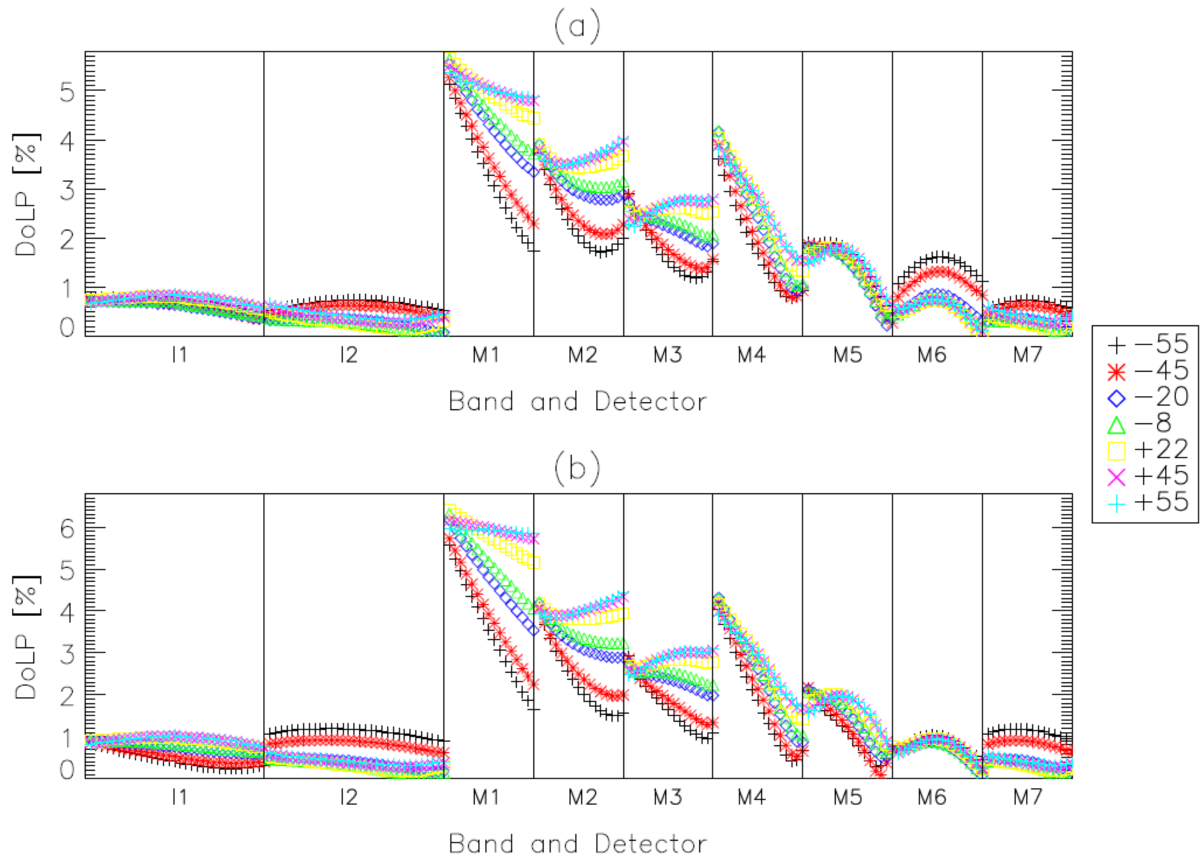

Figure 4: *DoLP* [%] results derived from FP-11 testing. The different color / symbol combinations correspond to the different measured scan angles, as shown in the legend. The x-axis shows each band demarked by vertical solid black lines; within each band the *DoLP* for each detector is plotted in ascending order along the x-axis. Plot (a) shows the results for HAM side 0 and plot (b) graphs the results for HAM side 1.

8. NOAA/NASA ADDITIONAL POLARIZATION TEST RECOMMENDATION

VIIRS/J1 polarization response test results and NASA modelled impacts to EDRs were reviewed and discussed by NASA and NOAA scientists. In an effort to fully characterize the impact of the polarization sensitivity and to ultimately enable high-fidelity on-orbit corrections, the NASA/NOAA group recommended two additional sets of polarization measurements to be performed in ambient at Raytheon. These measurements included the following:

- polarization sensitivity of bands M1 to M7 at 4 additional VIIRS scan angles using polarized SIS-100 output. For each band, the polarization sensitivity was requested to be measured at VIIRS scan angles of +4, -15, -30, and -37 degrees. Measurements at -8 degrees were also requested as a scan angle common to previous polarized SIS-100 measurements made by Raytheon.
- polarized radiance response as a function of wavelength of bands M1 and M4 using monochromatic polarized T-SIRCUS light. For each band, 13 wavelengths were requested to be measured, with 3 wavelengths near the band center and 5 wavelengths on each side of the band center. These measurements were to be made at 2 VIIRS scan angles for each band. At each wavelength and at the two scan angles, measurements, by VIIRS, of the polarized output of the T-SIRCUS were to be made at 13 polarization angles from 0 to 180 degrees in steps of 15 degrees.

The data from the measurements at the additional scan angles would be used to validate the consistency and smoothness of the polarization sensitivity data previously acquired by Raytheon and would provide confidence in post-launch EDR corrections. The radiance response measurements would be used to quantify the effect of polarization on the shape of VIIRS response curves and validate the predictions of the Raytheon VIIRS/J1 polarization response model for those bands. The Raytheon model would be used to determine polarization effects at scan angles not measured in ambient conditions at Raytheon, evaluate impacts from polarization changes in band spectral shape, and identify causes of on-orbit changes in polarization sensitivity.

9. FRED MODEL AND ITS PREDICTIONS

A model of the VIIRS/J1 optical system, as shown in Fig.1, was used in the FRED optical analysis program. The optical prescription used in this model is identical to the SNNP model[17]. In the J1 model the mirror coatings are virtually the same as in the SNNP model. Fig. 5a shows the difference between the s and p reflectance $(R_s-R_p)/2$ (which is a measure of polarization sensitivity and is equal to the unpolarized transmittance * linear diattenuation) of the J1 mirrors and SNNP mirrors. However, the difference between s and p transmittance $(T_s,T_p)/2$ of the J1 Integrated Focal plane Assembly (IFA) filters, Fig. 5b-i, is significantly higher than the SNNP filters, especially at the edges of the spectral bands. This difference is an unintended consequence of the redesign of the filters between SNPP and J1 (which was done to improve manufacturability and equalize the response across the VISNIR bands) and is significant even at an Angle of Incidence (AOI) of 13 degrees, which is the highest angle the in-field ray bundle makes with the IFA. Though the phenomenon of polarization splitting at the edges of bandpass filters has been documented[18], an assumption was made that this would not be a significant effect in VIIRS because of the low AOI on the IFA, and therefore there was no component-level specification for maximum allowed polarization splitting was defined for it. As shown in Fig. 6 this increase in polarization splitting for J1 significantly increases its polarization sensitivity relative to SNNP, especially for the M1-M4 bands. The figure shows that the model accurately predicts the J1 polarization sensitivity to within 1.6 % in band-averaged *DoLP*. To achieve this accuracy, it was necessary to sample each waveband with 25 wavelengths across each waveband, as measured from the 5 % unpolarized transmittance points. The predicted polarization sensitivity vs. wavelength is shown in Fig. 6; this data is necessary for calibrating the sensor's Relative Spectral Response (RSR)[19].

5a 5b 5c 5d 5e

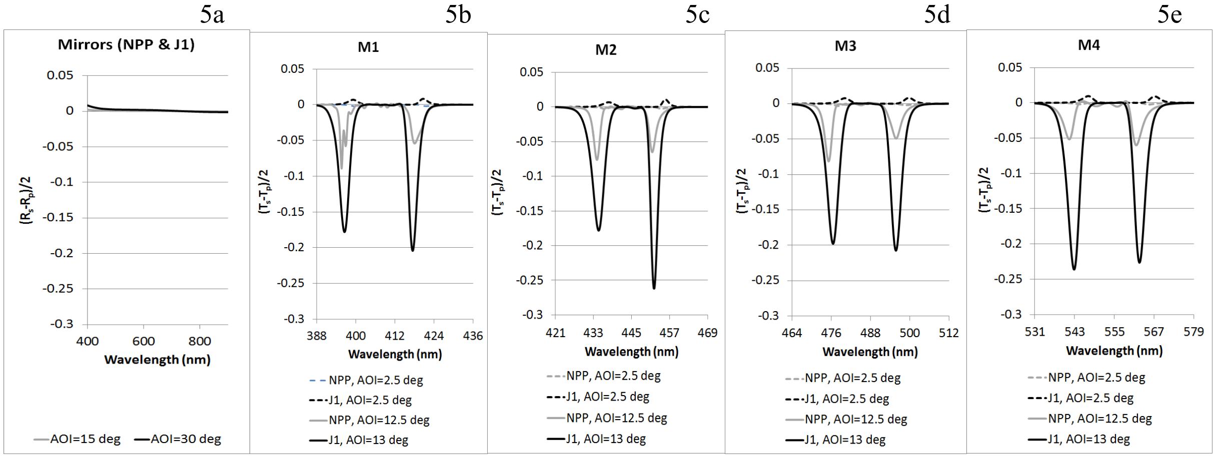

5f 5g 5h 5i

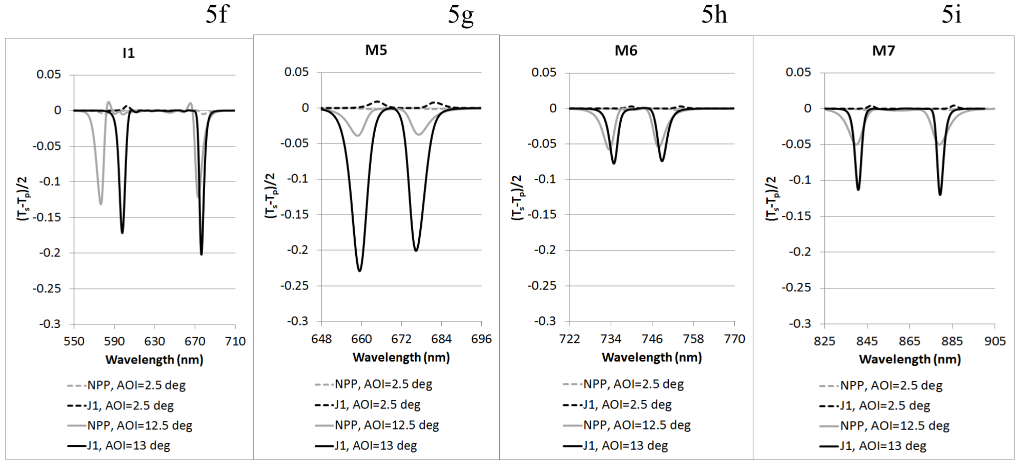

Figure 5: Predicted $(R_s-R_p)/2$ of the SNNP and J1 mirrors, and $(T_s-T_p)/2$ of the SNNP and J1 IFAs.

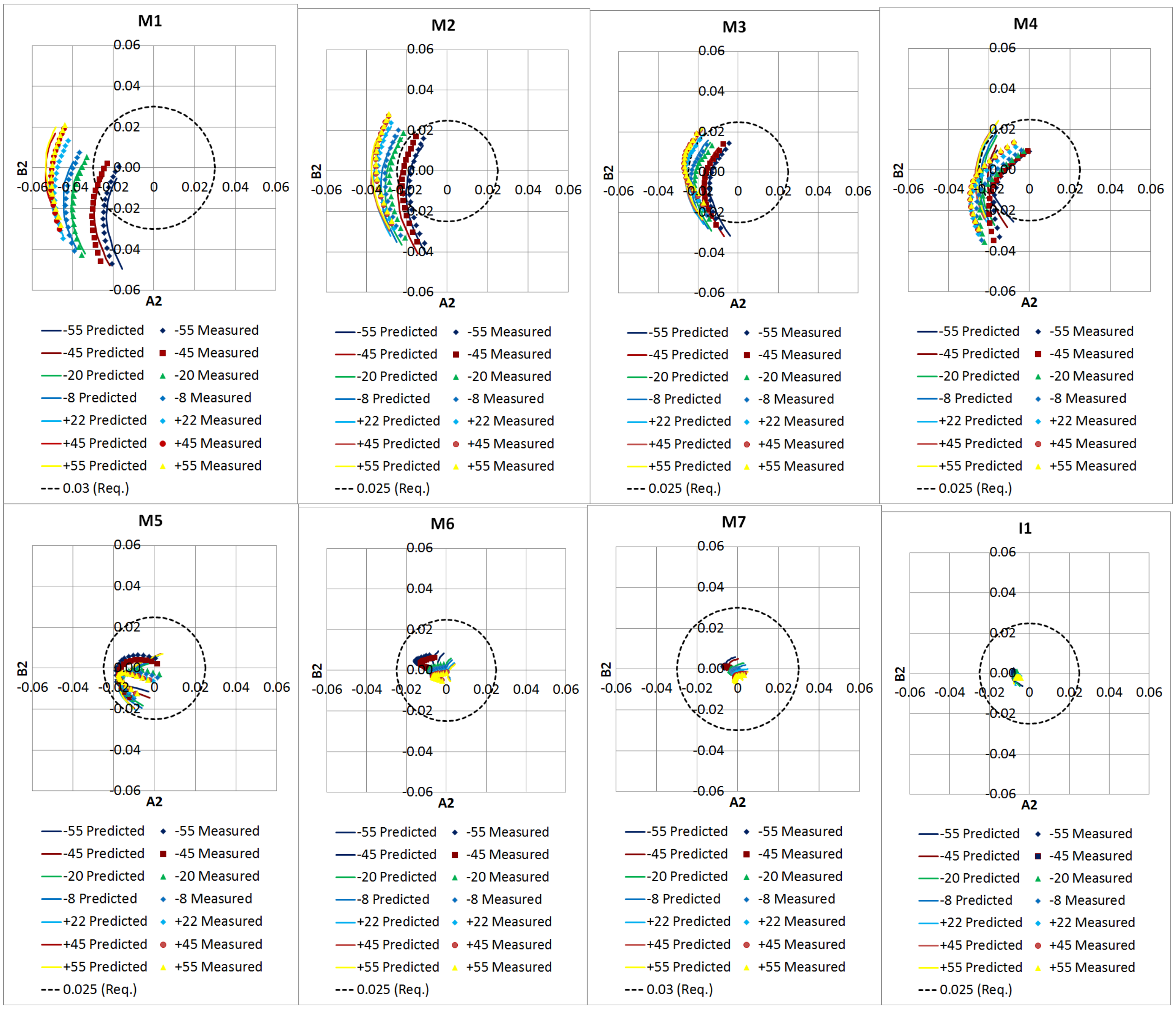

Figure 6: Predicted and Measured HAM 1 J1 Polarization Sensitivity (Spectral Band-Averaged). The predictions are made using the product of the measured spectra of the SIS(100)-2 and either the Sonoma bandpass filter, and BVO777™ polarizer (bands M1 to M3 only) or the BVONIR™ polarizer (M4 to M7) used in the FP-11 test.

In the analysis performed for SNNP[17], only the center wavelength of each waveband was used, and this resulted in an error between the predicted and measured polarization sensitivity. When the analysis was run using 25 wavelengths per band the result is a much better correlation (<0.5 % for most bands) between the predicted and measured polarization sensitivity.

10. ANALYSES AND ACTIVITIES BETWEEN FP-11 AND FP-11' AND T-SIRCUS

It has been generally accepted that the TOA correction for ocean color data products should work if the sensor polarization response is relatively small and has been characterized to within 0.5 % uncertainty (i.e., within instrument requirements).[20] However, although VIIRS/J1 characterization uncertainty for polarization response was claimed to be within this uncertainty threshold, the response observed for this sensor exceeded instrument requirements, and in some cases exceeded that of heritage sensors (especially for band M4). In addition, the FRED model was predicting changes in instrument spectral response with the polarization state of incoming light. It was apparent that spectral response changes could further degrade the correction effectiveness.

To place an upper bound on the potential impact of characterization error to ocean color products, VIIRS/SNNP scenes were selected as stressing cases for sensitivity to characterization error. Each scene was processed to produce EDR values, with and without simulated characterization errors. The resulting errors in the EDR values were used to test the assumption that the characterization uncertainty was adequate in the worst case.

Changes observed in the TOA radiances to perturbations in the polarization characterization were less than 0.2 %, with the highest change occurring in band M1. This small effect is expected given that the largest characterization uncertainty provided was 0.38 % (see Table 2), which would apply to completely linearly polarized light. The actual maximum degree of polarization of the TOA radiance is usually less than 70 %.

The EDR quantities evaluated include water leaving radiance and chlorophyll *a* concentration. Responses to simulated one-sigma errors, as predicted using Table 2 uncertainties, were estimated for open-ocean and coastal cases (see Fig. 7). For the open ocean, the water-leaving radiances were affected by less than 5 % for the blue bands, more for green and red bands. For the coastal case, the M1 water-leaving radiance was affected most (up to 10 %). Both the magnitude and the spectral dependence of the impact of the disturbance were in line with expectations. Chlorophyll *a* concentration for the open ocean changed by more than 10 % for less than 0.3 % of the retrievals, and by 0.01 mg m^{-3} for less than 0.02 % of the retrievals. For the coastal case, chlorophyll-a concentration changed by more than 5 % for less than 1.1 % of the retrievals (with no change larger than 10 %), by 0.01 mg m^{-3} for about 70 % of the retrievals, and by 0.1 mg m^{-3} for about 1 % of the retrievals. In general, the results showed little effect to the reported uncertainties.

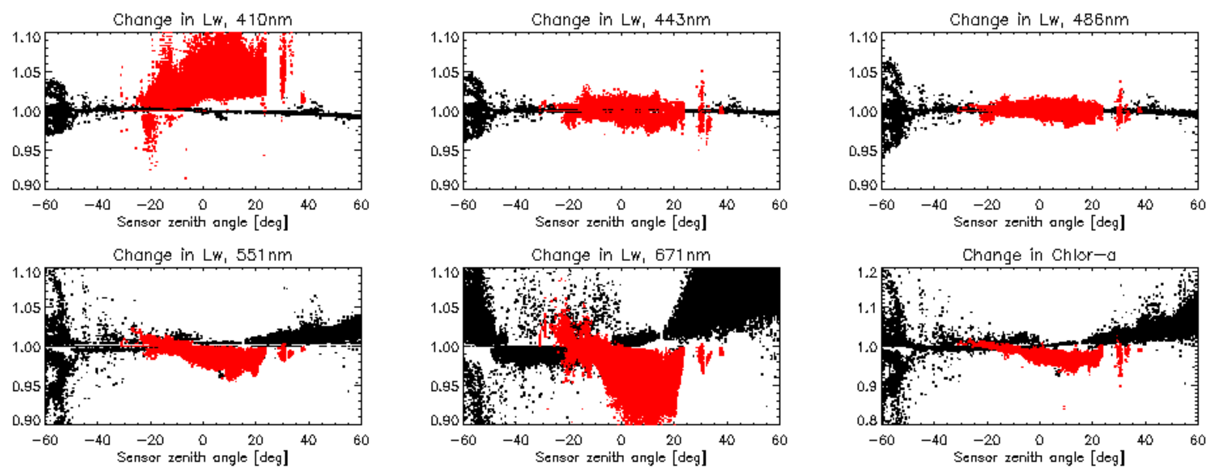

Figure 7: Ratio of perturbed EDR or Level-2 products to base case. These plots illustrate the relative change induced by the simulated highly stressing, but rare error condition as a function of sensor zenith angle. The red markers represent the coastal results, the black represent the open ocean results.

To evaluate the spectral effects, the spectral response predicted by the FRED model was applied to two different spectral shapes, one representing Rayleigh (atmospheric molecular) scattering and one representing a 2300°K blackbody source. The results indicated that changes in measured radiance (either on orbit or in laboratory) were generally small, but do span a significant range of about 1 % for M1 down to about 0.3 % for M7. More importantly, the resulting relative percent changes from these two spectra were anti-correlated, potentially aggravating the effects when applying prelaunch calibration to TOA measurements. The model predicted that most of polarization response comes from the edges of the band pass. Thus, the anti-correlation was likely caused by the opposite signs of the slope for spectral shapes, which would emphasize opposite sides of the band pass. This suggests that although different source spectra may yield an overall uncertainty within 0.5 %, they can still systematically disagree on a larger scale.

Spectral effects could be a significant source of uncertainty in the polarization correction. Systematic effects arising from the spectral shape differences between the TOA spectrum and source used in tests could lead to significant additional striping. Thus it was recommended that polarization correction coefficients used for on-orbit measurements be based on a source spectrum with a similar spectral shape to the Rayleigh spectrum. More importantly, these results underscored the need for verification of the FRED model predictions through the SIRCUS testing of the instrument.

11. SECOND POLARIZATION TEST FP-11'

The second VIIRS polarization test, FP-11', took place in Raytheon SAS in El Segundo in the 4th quarter of 2014. The test configuration was the same as in FP-11. The polarization sensitivity test results[16], including the repeated measurement at -8^o scan angle, are shown Fig. 8. The polarization sensitivity measurement at -8^o scan angle between FP-11 and FP-11' was very similar. The small differences at -8^o scan angle between FP-11 and FP-11' results is consistent with estimated polarization measurement accuracy.

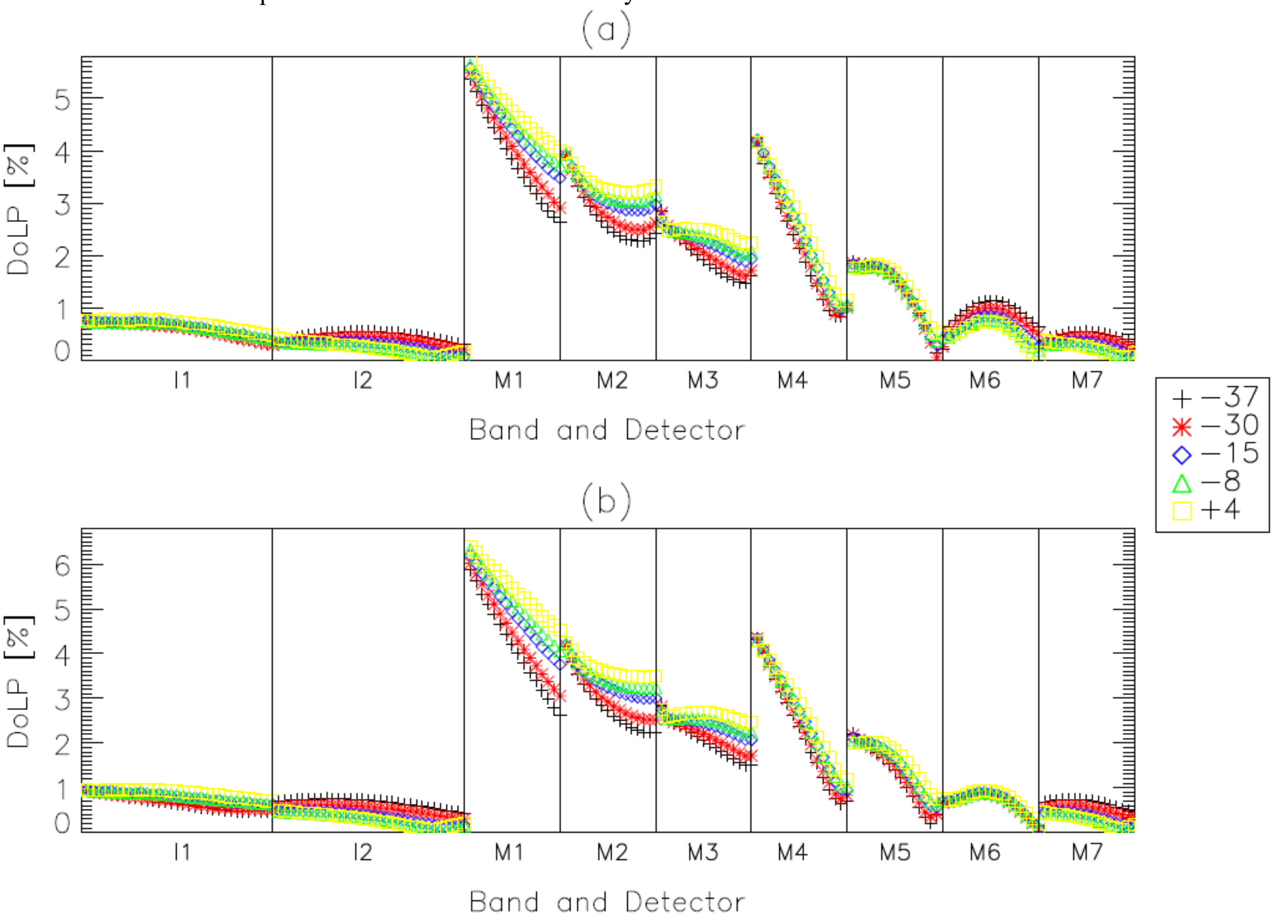

Figure 8: *DoLP* [%] results derived from FP-11' testing. The different color / symbol combinations correspond to the different measured scan angles, as shown in the legend. The x-axis shows each band demarked by vertical solid black lines; within each band the *DoLP* for each detector is plotted in ascending order along the x-axis. Plot (a) shows the results for HAM side 0 and plot (b) graphs the results for HAM side 1.

12. VIIRS SCAN ANGLE INTERPOLATION

VIIRS on-orbit data analysis requires knowledge of the polarization sensitivity at all scan angles. However the ground characterization (FP-11) measured the polarization at only the following scan angles:

$$-54.83^o, -44.92^o, -19.85^o, -7.94^o, -7.94^o, -7.94^o, 21.95^o, 45.06^o, 54.99^o.$$

(The repeated angles indicate measurements made at the same scan angle as checks on measurement repeatability.) Interpolation is required for other angles. The interpolation is accomplished by fitting a second order polynomial to the two theta Fourier coefficients *A2* and *B2* (corrected by A0) for each detector. These *A2* and *B2* coefficients (defined in Appendix) are used to calculate the DoLP and phase for each spectral band, detector, at all scan angles.

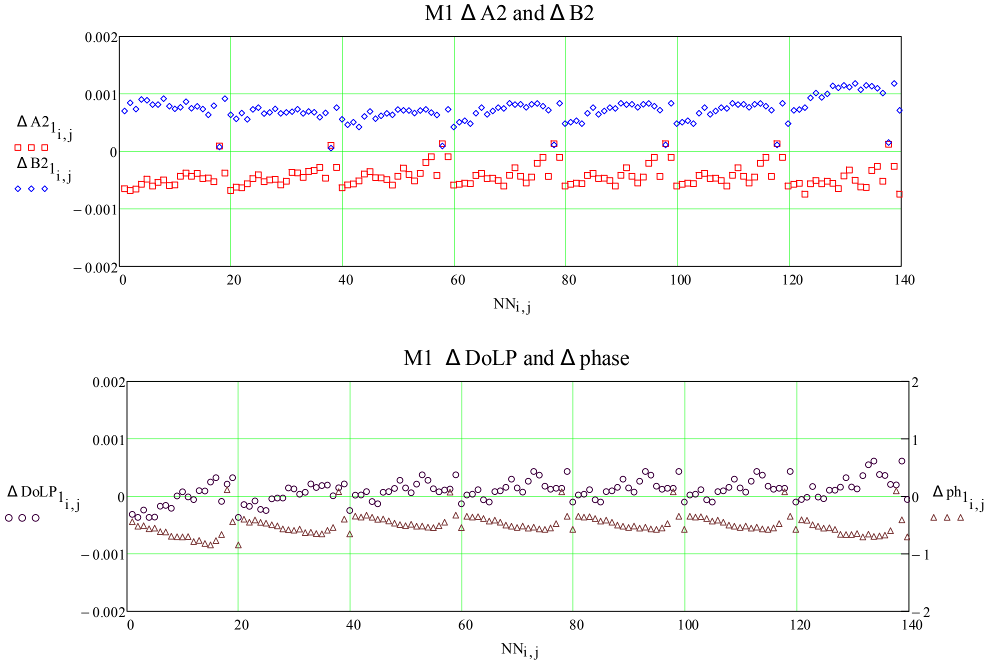

Figure 9: Band M1 differences between FP-11 and FP-11' *A2* and *B2* (Mueller matrix elements) and *DoLP*

It was found that the second order polynomial fit to the measured *A2* and *B2* over the all scan angles had residuals of less than 0.001. Since this fit is a critical parameter, it was decided that an additional test was needed to validate the FP-11 results. The second instrument polarization measurement, FP-11', used the same FP-11 polarization test equipment, but the measurements were performed at the following different scan angles:

$$-36.99^{o}, -29.98^{o}, -15.02^{o}, -7.98^{o}, -7.98^{o}, -7.98^{o}, 4.00^{o}.$$

The FP-11 *A2* and *B2* polynomials were used to calculate the *DoLP* and phase at the FP-11' scan angles. In addition, FP-11' *A2*' and *B2*' polynomials were used to calculate the *DoLP*, and phase at measured FP-11' scan angles. The differences between the two sets of *A2*, *B2*, *DoLP* and phase were calculated and plotted in Fig. 9, showing the results for spectral band M1. The major tick marks on the abscissa delineate the seven FP-11 scan angles and the points between the tick marks are the data for the 16 M1 detectors and the mean, std dev, max and min.

Use of FP-11 *A2* and *B2* polynomials has shown that VIIRS polarization performance can be predicted at intermediate scan angles: *A2* values are within +/- 0.001 and *B2* values are within +/- 0.001. In general, the *DoLP* is within +/-0.0005 except for M4 which is within +0.0005 to -0.0013 and for band M5 the variation is within 0 to -0.001.

13. T-SIRCUS SET UP AND OPERATION

The T-SIRCUS system, the traveling version of the Spectral Irradiance and Radiance Calibration using Uniform Sources facility[21,22], was developed by NIST to radiometrically calibrate instruments at higher spectral brightness than possible with prior lamp and monochromator based techniques. It consists of, Fig. 10, an integrating sphere for generating uniform illumination, high accuracy transfer radiometers, fiber coupled tunable laser based light sources, and control and monitoring electronics.

For the VIIRS polarization sensitivity tests using the T-SIRCUS, a 101.6cm (40") diameter SIS with a 30.48cm (12") circular exit port was used to generate a monochromatic light illumination which overfill VIIRS's aperture while a transfer radiometer mounted directly to the sphere serves as a radiance monitor and provides feedback for a laser power stabilizer. Using the sphere monitor as a feedback source rather than sampling a portion of the free space beam improves stability as it compensates for variations in fiber coupling due to vibration. The correspondence between radiance at the output port of the sphere and monitor position was checked both before and after instrument calibration by comparing response between the sphere monitor and a second transfer radiometer mounted in front of the sphere. The radiometers are of the silicon trap detector type and are temperature stabilized during measurements. They were calibrated over the wavelength range of interest using absolute radiometric facilities at NIST.

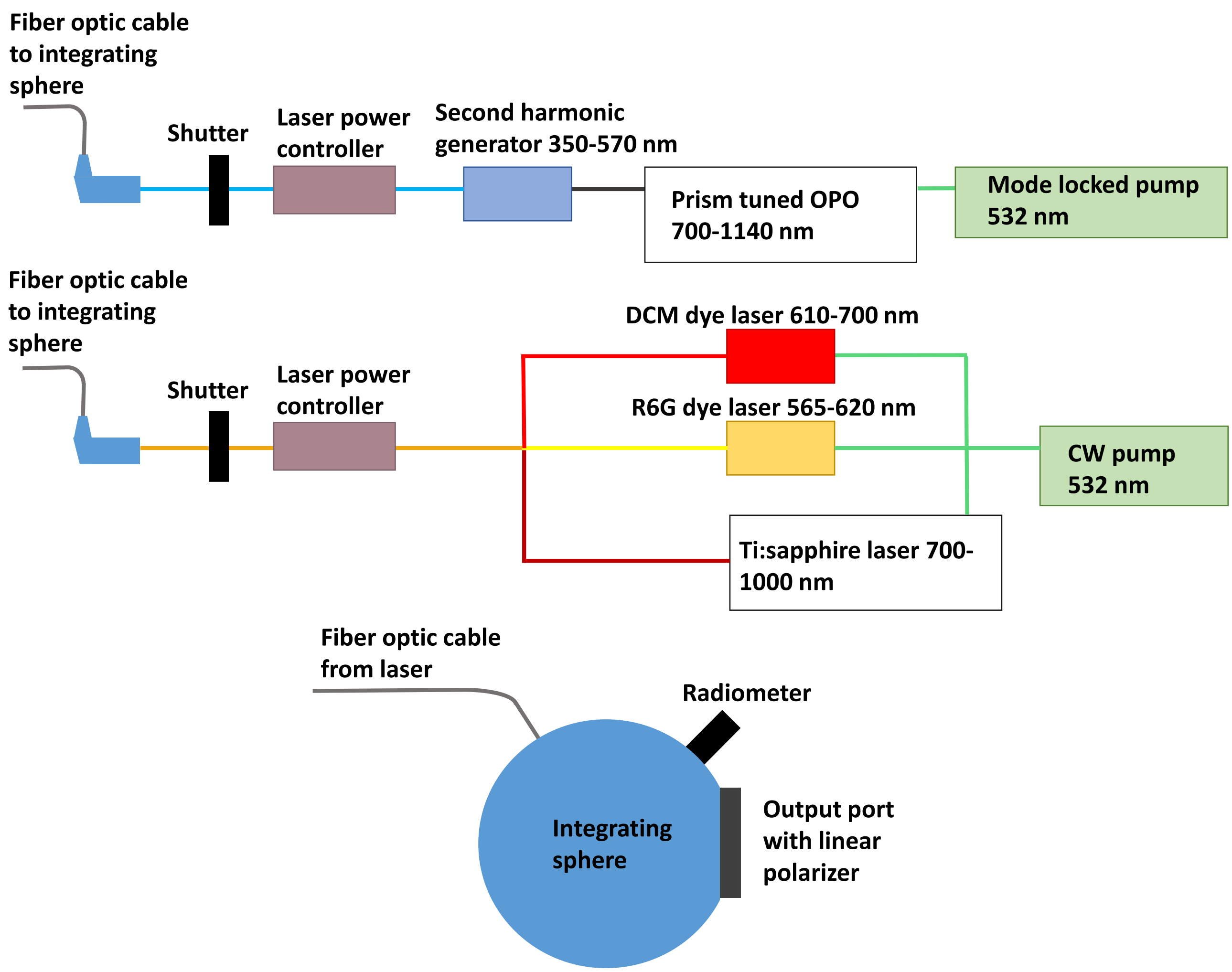

Figure 10: T-SIRCUS set up

Several lasers and optical parametric oscillators were used to tune across the spectrum. The short end of the wavelength range from 350 nm to 570 nm was covered with the second harmonic of a custom optical parametric oscillator developed at NIST and pumped at 532 nm by a 20 watt frequency doubled $Nd:VO_4$ laser. The pump laser is mode-locked, providing pulses of several picoseconds duration at 80 MHz repetition rate. The oscillator output is therefore also pulsed at 80 MHz, but is treated as continuous wave during the calibration as it is well above the instrument frequency response. The integrating sphere also provides some temporal averaging of pulses. There is a small tuning gap near 532 nm when the oscillator is operating near its degeneracy of 1064 nm, but this is in an out of band region of VIIRS where small tuning steps were not needed.

The remainder of the visible spectrum is covered with two dye lasers; Rhodamine 6G for 565 nm to 620 nm and DCM for 610 nm to 700 nm. Both were pumped by an 18 watt continuous wave frequency doubled $Nd:VO_4$ laser. This laser also served as the pump source for a titanium sapphire laser which covered the remainder of the spectrum from 700 nm to 1000 nm.

14. T-SIRCUS (MONOCHROMATIC) SPECTRAL POLARIZATION MEASUREMENT

The reason for performing monochromatic polarization measurements of VIIRS has its roots in the fact that the VIIRS J1 optical filters were redesigned from SNNP filters to reduce out-of-band effects. The redesigned filters have, as it turns out, significant polarization across the spectral band, in particular at the spectral band edges. (The "S" and "P" transmission at the spectral band edges differ.) When the Raytheon polarization model, as described above, takes this into account, the model prediction and FP-11 and FP-11' results for band M1 is agree well, but for band M4 the agreement could be better. To check the correctness of the J1 model's predictions and increase the confidence that the J2 focal plane filters (redesigned with the aid of the polarization model to reduce the band edge polarization) would result in less polarization sensitivity, polarization measurements using monochromatic light generated from the T-SIRCUS were performed. Since polarization measurement using a monochromatic light provides wavelength specific polarization sensitivity measurement (as oppose to band averaged polarization sensitivity when white illumination light source was used), T-SIRCUS polarization measurements would provide additional information to understand the effect of TOA and SIS(100)-2 spectral distribution to VIIRS on-orbit polarization performance.

The T-SIRCUS polarization measurements were performed for two bands, M1 and M4, and at two scan angles, – 8^{o} and +45^{o}. The main reason for this choice was that band M1 showed largest polarization sensitivity, but agreed reasonably well with FRED™ model, while for band M4 (important for the ocean color community and accurate correction for instrumental polarization is required) measured polarization sensitivity showed the largest relative discrepancy with FRED model predictions. Initially, 13 monochromatic polarization measurements were to be performed for each band, with five wavelengths on the band edges and 3 on the band plateau. But as M4 testing progressed, 4 additional plateau measurements for band M4 were added to confirm the presence of polarization variation on the band plateau not seen in both the bandpass focal plane filter measurements and consequently the FRED™ model.

With the T-SIRCUS test data in hand, a fourth order Fourier series was used to fit the sensor response over polarization angle. The Fourier components were used to determine the *DoLP* and phase angle. This was done separately for each detector, wavelength, and scan angle. The Fourier components were weighted by the spectral transmittance of the system, and then integrated over the bandpass to determine the band dependent *DoLP* and phase angle for comparison to FP-11 / FP-11' polarization measurements. A more extensive discussion of the T-SIRCUS results are in "Analysis of JPSS J1 VIIRS Polarization Sensitivity Using the NIST T-SIRCUS".

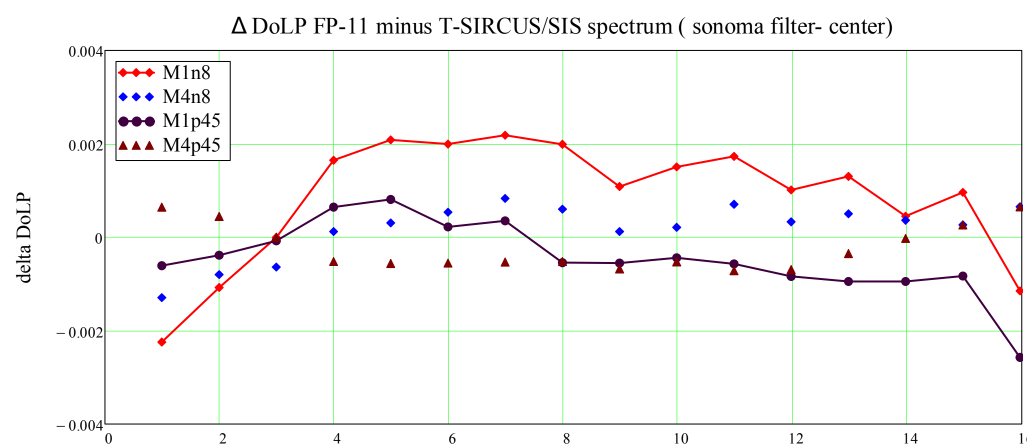

Figure 11: Band M1 and M4 detector number

A summary of T-SIRCUS measurement results is as follows:

1. T-SIRCUS data illustrates enhanced polarization at band edges similar to the Raytheon FRED™ polarization model predictions.

2. The poor model correlation for band M4 might be due to inadequate polarization characterization of the component.
3. VIIRS polarization performance characterization has a dependency on source spectral distribution ranging between 0.0035 and 0.0010.
4. Based upon the analysis, T-SIRCUS polarization, after correction for SIS100-2 spectral effects agree with FP-11 results within +/-0.002, in Fig. 11, but because of the sparse sampling and depending on how the data is filtered[23], can be +/-0.005.

15. T-SIRCUS MEASUREMENT RESULTS[24]

Based on T-SIRCUS test data, a fourth order Fourier series was used to fit the sensor response over polarization angle. The Fourier components were used to determine the *DoLP* and phase angle. This was done separately for each detector, wavelength, and scan angle. The Fourier components were weighted by the spectral transmittance of the system, and then integrated over the bandpass to determine the band dependent *DoLP* and phase angle for comparison to FP-11 / FP-11' polarization measurements.

The measured dn (offset corrected detector response) for each polarizer angle at 408 nm is shown in Fig. 12(a) for all detectors (at +45 degrees scan angle, HAM side 1); the symbols represent the measured dn and the solid lines denote the calculated Fourier series. Each detector is represented by a different symbol / color as defined in the legend. Similarly, the measurements and fits for 421 nm, 546 nm, and 559 nm (at +45 degrees scan angle, HAM side 1) are shown by the symbols and solid lines in figs. 12(b, c, and d). Note that the lines fit the data very well and closely follow a two-cycle oscillation. This indicates that the second order Fourier components dominate. Note that there is considerable variation for some wavelengths in terms of both amplitude and phase angle. The cases shown in Fig. 12 are indicative of all the T-SIRCUS measurements.

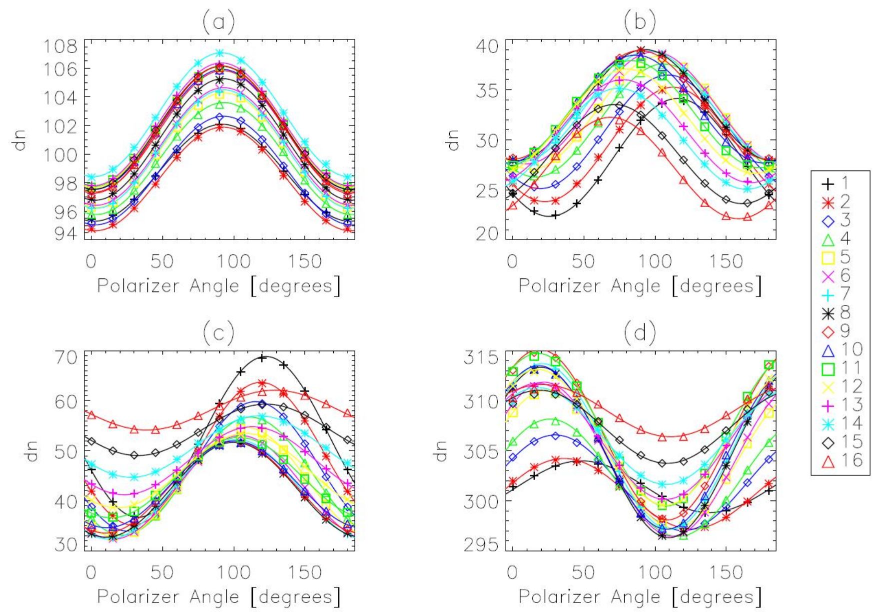

Figure 12: Measured dn versus polarizer angle [degrees] for M1 at 408 nm (a), M1 at 421 nm (b), M4 at 546 nm (c), and M4 at 559 nm (d) at +45 degrees scan angle, HAM side 1. The legend defines the different symbol / color combinations which correspond to each detector.

The spectrally weighted *DoLP* for M1 (+45 degrees scan angle, HAM side 1, resampled to 1 nm) as a function of wavelength is shown in Fig. 13(a) indicates that the *DoLP* increases on the sides of the bandpass, and then decreases in the middle. A similar plot for M4 (+45 degrees scan angle, HAM side 1, resampled to 1 nm) is shown in Fig. 13(b). For the M4 case, the *DoLP* oscillates in the center of the bandpass; the minimums in *DoLP* correspond to phase angle shifts. The cases not shown (M1, -8 degrees scan angle, HAM side 1; M4, -8 degrees scan angle, HAM side 0; and M4, -8 degrees scan angle, HAM side 1) show similar results. The corresponding ray trace model results are shown in figs. 13(c) and 13(d) for M1 and M4, respectively. Note that the model and measurements agree in the general shape and characteristics of the *DoLP* versus wavelength. For M1, the modeled bandpass is slightly wider than the measurement; for M4, the modeled bandpass is also wider and the phase angle shifts that occur in the center of the bandpass were not captured by the model.

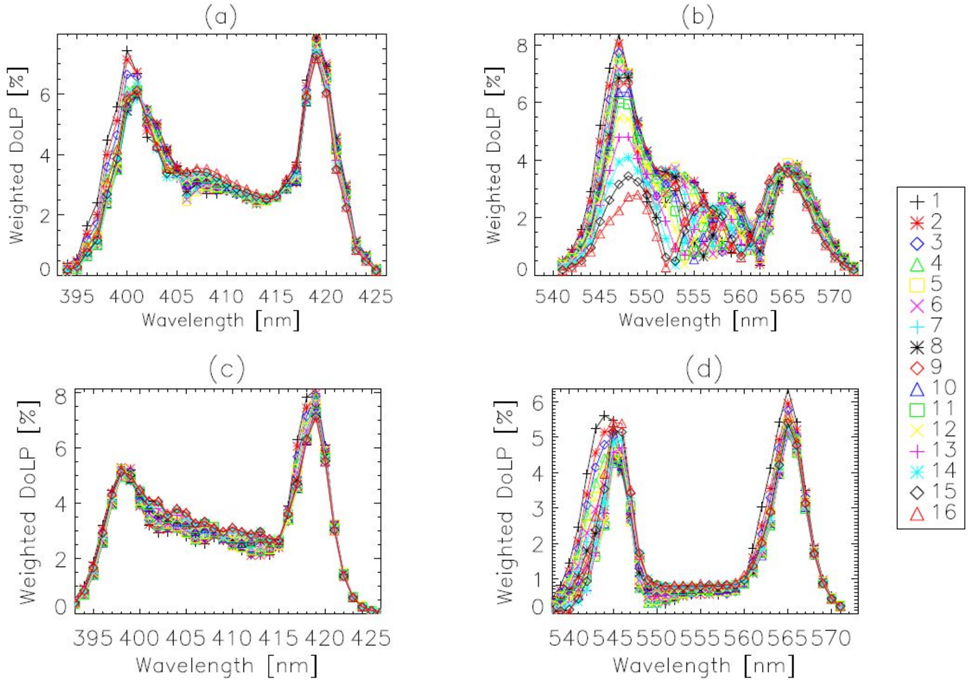

Figure 13: Measured, spectrally weighted *DoLP* versus wavelength for M1 (a) and M4 (b); modeled weighted *DoLP* versus wavelength for M1 (c) and M4 (d). All plots show data at +45 degrees scan angle, HAM side 1. The legend defines the different symbol / color combinations which correspond to each detector.

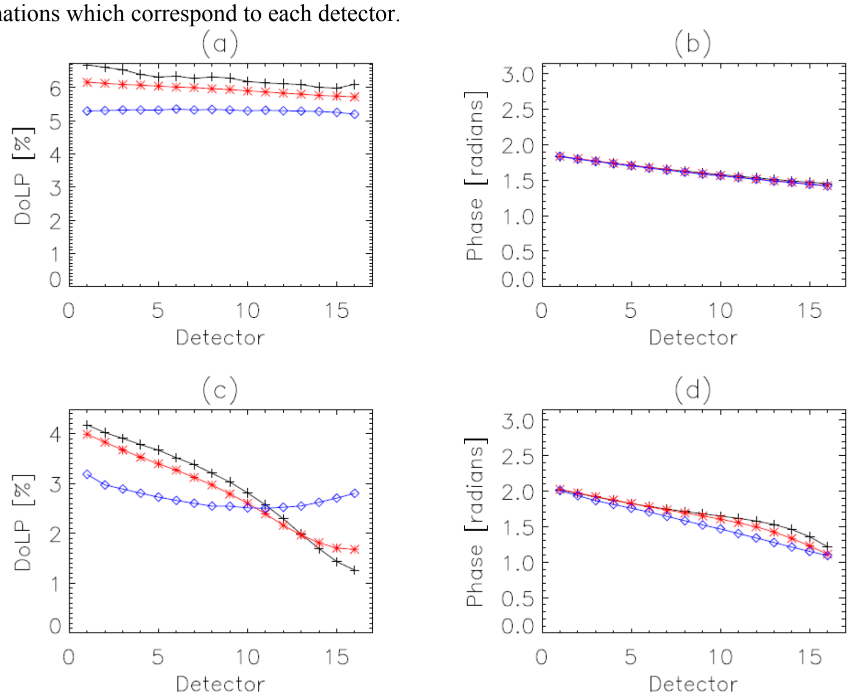

Figure 14: Plots of the *DoLP* and phase showing: M1 at +45 degrees scan angle, HAM side 1 in (a) and (b) as well as M4 at +45 degrees scan angle, HAM side 1 in (c) and (d). Black '+'s indicate T-SIRCUS measurements, red '*'s denote broadband measurements, and blue '◊'s refer to the model.

The band dependent *DoLP* and phase angles are shown for +45 degrees scan angle, HAM side 1 in Fig. 14 (all other cases show similar results). In general, the T-SIRCUS results agree reasonably well with the broadband measurements, with differences of up to about 0.5 %. Note that the M1 and M4 bandpasses were not critically sampled (the laser bandpass was less than 1 nm). Model differences with measurements are small for M1, but larger for M4; for M4, the detector dependence was not captured well by the model. The phase angles are very similar for the M1 cases; however, for M4, the phase angle differences between T-SIRCUS and broadband measurements were larger for higher number detectors, up to about 14 degrees.

16. CONCLUSION

The polarization sensitivity measurement of the VIIRS/J1 instruments, FP11, was performed. While polarization characterization uncertainty was less than 0.38 %, the maximum polarization sensitivity for M1, M2, M3, and M4 bands was measured to be 6.4 %, 4.4 %, 3.1 %, and 4.3 %, respectively, exceeding the specification. The polarization sensitivity measurement of VIIRS/J1 AOA has similar magnitude of polarization sensitivity for M1 to M4 bands.. The FRED™ polarization ray trace model indicated the increased polarization sensitivity for M1 to M4 bands was mainly due to the S and P polarization split at the leading edge and the trailing edge of newly manufactured focal plane spectral bandpass filter in front of the VISNIR detectors. The polarization sensitivity of M1 and M4 bands were measured on the edges and peak of the bandpass filter using a monochromatic light from the T-SIRCUS which confirmed the FRED™ model's predictions. To improve the confidence in the polarization scan angle interpolation, VIIRS/J1 polarization measurement were performed at additional scan angles, FP-11', using a white illumination light source. The repeatability of polarization sensitivity at -8^{o} scan angle between FP-11 and FP-11' was consistent with polarization measurement uncertainty. In general, polarization sensitivity vs. scan angle interpolation uncertainty was determined to be less than +/- 0.001. The good agreement between the FRED model, FP-11, FP-11' and the T-SIRCUS measurements increases the confidence in the FRED™ model and its use to predict future on-orbit polarization performance and its ability (with suitable coating file updates) to predict J2 performance. Given the results of these measurements, VIIRS/J1 will need a separate atmospheric correction for each detector and not just for a single band dependent correction for the entire 16-element detector array.

17. ACKNOWLEDGEMENTS

The authors wish to thank the VIIRS operations crew, who control the workings of VIIRS during the polarization tests for their patience and willingness to explain what was going on during the tests. Thanks also go to Jolene Vallejo for her administrative help. Also thanks go to JPSS management for their support of this work.

18. APPENDIX

Table A1. Translation between VIIRS and Mueller Matrix terminology

VIIRS Terminology	Mueller Matrix Terminology	Comments
Polarization sensitivity or Degree of Linear Polarization (*DoLP*)	Linear Diattenuation	$DoLP$=sqrt($A2^2$+$B2^2$)
A2 Fourier Coefficient	Mueller matrix element m_{12}	
B2 Fourier Coefficient	Mueller matrix element m_{13}	
Phase Angle	Angle of Linear Diattenuation	Phase Angle=0.5*$\tan^{-1}$($B2/A2$)

REFERENCES

[1] Schueler, C., Clement, J. E., Ravella, R., Puschell, J. J., Darnton, L., DeLuccia, F., Scalione, T., Bloom, H., and Swenson, H., "VIIRS Sensor Performance", Geoscience and Remote Sensing Symposium, 2003. IGARSS '03. Proceedings. 2003 IEEE InternationalYear: 2003, Volume: 1, Pages: 369 - 372 vol.1

[2] Novitisky, E.J., Herbst, S., Young, J.B., Puschell, J.J., Fest, E.C., Guenther, B.," Polarization sensitivity of Visible Infrared Imager Radiometer Suite (VIIRS) Flight Unit 1", Proc. SPIE **8516**, Remote Sensing System Engineering IV, 851601 (October 23, 2012)

[3] Sun, J., “Polarization sensitivity analysis of VIIRS F1 VisNIR bands,” Unpublished (2010)
[4] Waluschka, E., “VIIRS polarization testing", Proc. SPIE **7452**, 745209 (2009)
[5] Goldstein, D., Polarized Light, 2nd. Ed., Chapter 9, Marcel-Dekker (2003)
[6] Novitsky, E.J., “J1 AOA Polarization Characterization – Test and Results”, Raytheon ENB VIIRS.03.08.044, Unpublished (2012)
[7] Waluschka, E., Mathcad - ETP078 data - Error bars for TC100-101 and TC49-59 dolp with BVONIR correction factor TC33.pdf, Unpublished, (2012)
[8] Young, J., “J1 AOA Polarization Comments.pptx”, Unpublished (2012)
[9] Bolder Vision Optik, 4730 Walnut Street, Suite #102, Boulder, Colorado, 80301
[10] MOXTEK, Inc., 452 W 1260 N, Orem, UT 84057
[11] Sonoma C165-210-JB NIR Blocking Filter, Sonoma Photonic Incorporated, 1750 Northpoint Parkway, Santa Rosa, CA
[12] Raytheon, Performance Specification, Sensor Specification for the VIIRS, PS154640-101 Rev. D, Unpublished (2008)
[13] Meister, G., Kwiatkowska, E. J., Franz, B. A., Pratt, F. S., Feldman, G. C., and McClain, C. R., “Moderate-Resolution Imaging Spectroradiometer ocean color polarization correction,” Appl. Opt. **44,** 5524 – 5535 (2005)
[14] Gordon, H. R., Du, T., and Zhang, T., “Atmospheric correction of ocean color sensors: analysis of the effects of residual instrument polarization sensitivity,” Appl. Opt. **36,** 6938 – 6948 (1997)
[15] Waluschka, E., “MODIS polarization measurements and simulation and the 4θ effect", Proc. of SPIE **3121**, 278 (1997)
[16] Moyer, D., McIntire, J., Waluschka, E., Xiong, X., and DeLuccia, F., “JPSS-1 VIIRS pre-launch polarization testing and performance,” IEEE T. Geosci. Remote (2015). In press.
[17] Fest, E., “VIIRS polarization sensitivity testing and analysis”, Proc. of SPIE **7461**, 746102 (2009)
[18] Miller, R. and Hennessey, G., “Infrared coatings for 2-15 micron”, Proc. of SPIE **0050**, 119 (1974)
[19] Moeller, C., Schwarting, T., and Moyer, D., “JPSS J1 T-SIRCUS RSR,” Unpublished (2015)
[20] Meister, G. and Turpie, K.R., “Impact assessment of the polarization non-compliances discovered during J1 VIIRS prelaunch characterization: Impact on Ocean Environmental Data Records (EDR)”, Unpublished (2014)
[21] Brown, S. W., Eppeldauer, G. P., and Lykke, K. R., “Facility for Spectral Irradiance and Radiance Calibrations using Uniform Sources,” Appl. Op. **45**, 8218-8237 (2006)
[22] Barnes, R. A., Brown, S. W., Lykke, K. R., Guenther, B., Xiong, X., and Butler, J. J., “Comparison of two methodologies for calibrating satellite instruments in the visible and near infrared,” Proc. of SPIE **7862**, 78620C (2010)
[23] VCST_TECH_REPORT_14_086 (v3), unpublished.
[24] McIntire, J., Young, J. B., Moyer, D., Waluschka, E., Oudrari, H., and Xiong, X., “Analysis of JPSS J1 VIIRS polarization sensitivity using the NIST T-SIRCUS,” Proc. of SPIE **9607** (2015). In press.